Electronic Supplementary Material (ESI) for ChemComm.

Supporting Information

Site-specific sulfur-for-metal replacement in silver nanocluster

Ya-Ge Wu,[‡a,b] Jia-Hong Huang,[‡b] Chong Zhang,[b] Xiang-Kun Guo,[a] Wei-Na Wu,[a] Xi-Yan Dong,[*a,b] Shuang-Quan Zang[*b]

[a] *College of Chemistry and Chemical Engineering, Henan Polytechnic University, Henan Key Laboratory of Coal Green Conversion, Henan Polytechnic University, Jiaozuo 454000, China.*

[b] *College of Chemistry, Zhengzhou University, Zhengzhou 450001, China.*

E-mail: dongxiyan0720@hpu.edu.cn; zangsqzg@zzu.edu.cn

Experimental Details

Materials and reagents.

All the chemicals and reagents used in our study were of commercially available reagent grade and were used as received without any additional purification, including silver nitrate ($AgNO_3$, Aladdin), benzyl mercaptan ($HSCH_2Ph$, Aladdin), triphenylphosphine (PPh_3, Aladdin), Tetrakis(triphenylphosphine)palladium ($Pd(PPh_3)_4$, Energy Chemical), sodium borohydride ($NaBH_4$, 99.9%, Sinopharm chemical reagent co.), 9,10-Dimethylanthracene (DMA, Energy Chemical). N, N-bis(diphenylphosphanylmethyl)-3-aminopyridine (3-bdppmapy) was synthesized as reported before.[1] All reagents were purchased from Tianjin Kemiou Chemical Reagent Co., Ltd..

Characterization.

The thermogravimetric analyses (TGA) of the as-synthesized nanoclusters were performed on a SDT 2960 thermal analyzer from room temperature to 400 °C at a heating rate of 10 °C/min under oxygen atmosphere. UV-vis absorption spectra were recorded with a U-2000 spectrophotometer, and solution samples were prepared using CH_2Cl_2 as the solvent. Solid UV-Vis diffuse reflectance spectra were recorded with Hitachi UH4150 spectrometer. Electron paramagnetic resonance (EPR) spectroscopy was performed using a Bruker EMX plus 10/12 system (equipped with an Oxford ESR910 Liquid Helium cryostat). X-ray photoelectron spectroscopy (XPS) measurements were carried out using a VG Scientific ESCALAB 250 system with an Al Kα (300 W) X-ray resource. Fourier transform infrared (FT-IR) spectra were recorded on a Bruker ALPHA II spectrometer. The far infrared (FIR) spectra were recorded on a BROKER TENSOR II spectrometer. ICP-OES measurements were carried out using the ICAP6000 SERIES spectrometer. EDS measurement was collected using Zeiss Sigma 500. The photoluminescence (PL) emission spectra were measured by using a Horiba FluoroLog-3 spectrofluorometer. Singlet oxygen was generated from Perfect Light PCX-50A Discover (power density was 80 mW/cm^2).

X-ray crystallography.

SCXRD measurements were performed using Bruker ApexII charge-coupled detector equipped with Mo-Kα radiation ($\lambda = 0.71073$ Å) for $\mathbf{Ag_{36}}$ and a Rigaku XtaLAB Pro diffractometer with Cu-Kα radiation (λ = 1.54184 Å) for **PdAg$_{35}$**. The structures were solved using intrinsic phasing methods (SHELXT-2015) and refined by full-matrix least squares on F^2 using OLEX^2, which utilizes the SHELXL-2018/3 module[2]. All hydrogen atoms were placed in their calculated positions with idealized geometries, and they possessed fixed isotropic displacement parameters.

Appropriate restraints and/or constraints were applied to the geometry, and the atomic displacement parameters of the atoms in the cluster were determined. All non-H atoms were located in the electron density and refined with anisotropic thermal parameters. Due disorder of the CF_3COO^-, FLAT restraints were applied to keep the planarity of F atoms; SADI and DFIX were applied to keep the distances of C–F (*ca.* 1.45 Å), C–C (*ca.*1.51Å) and F···F of the CF_3COO^- in reasonable range; SAME restraints were applied to keep similar configurations of CF_3COO^- ligands. Besides, DFIX restraints were applied to keep the distances of C=O (*ca.* 1.2 Å), and C–N (*ca.*1.45Å) of the DMF molecules in reasonable range; AFIX 66 restraints were applied to keep the standard six-membered ring configuration of the phenyl group in the ligands (PPh_3 and $PhCH_2S^-$). ISOR, DELU and SIMU restraints were used for some atoms, especially peripheral F atoms with large thermal motion. All structures were examined using the Addsym subroutine of PLATON[3] to ensure that no additional symmetry could be applied to the models. For **Ag$_{36}$**, a solvent mask has been used due to severely disorder of free solvent molecules around the cluster and diffract weakly. According to **PdAg$_{35}$** data without solvent mask and TG data, the solvent molecules (*ca.* 10 DMF and 2 H_2O) are removed through solvent mask in the refinement.

Detailed information with respect to the X-ray crystal data, intensity collection procedure, and refinement results for the entire cluster compounds are summarized in Tables S2-S4.

Preparation of $Ag^I(PPh_3)NO_3$ complex.

The $Ag^I(PPh_3)NO_3$ complex was prepared according to a previous report.[4] Specifically, $AgNO_3$ (0.17 g, 1 mmol) was dissolved in CH_3CN (5 mL). PPh_3 (0.29 g, 1.1 mmol) was dissolved in CH_3CN (10 mL) and added to the first solution in a dropwise manner under vigorous stirring (~1200 rpm) and the stirring was continued for 15 min. The resulting mixture was then filtered. The filtrate was slowly rotary evaporated under vacuum. The final product $Ag^I(PPh_3)NO_3$ was directly used in the next step (73.5% based on $AgPhCH_2S$).

Preparation of $[Ag_{34}(PhCH_2S)_{18}(CF_3COO)_9(DMF)_6]$.

$[Ag_{34}(PhCH_2S)_{18}(CF_3COO)_9(DMF)_6]$ nanoclusters were synthesized according to the previous report.[5] $AgPhCH_2S$ (0.2 g, 0.9 mmol), CF_3COOAg (0.3 g, 1.4 mmol) and 3-bdppmapy (0.2 g, 0.4 mmol) were dissolved in a mixed solvent of CH_2Cl_2, and DMF (1:1) with the addition of 10 μL NEt_3 under stirring. The red solution was slowly evaporated in room temperature. After twenty days 29.5 mg black hexagons was obtained (8.3% based on $AgPhCH_2S$).

Preparation of $[Ag_{36}(PhCH_2S)_{18}(CF_3COO)_{10}(DMF)_4(PPh_3)_2]\cdot 10DMF\cdot 2H_2O$.

Firstly, $PhCH_2SAg$ (0.2 g, 0.9 mmol), CF_3COOAg (0.3 g, 1.4 mmol) were dissolved in a mixed solvent of CH_2Cl_2 and DMF (1:1). Then, $Ag^I(PPh_3)NO_3$ (0.4 g, 0.9 mmol) were added to the above solution, after 30 minutes, $NaBH_4$ (1 mL) aqueous solution (0.5 mg mL^{-1}) was added quickly to the above mixture. The reaction was allowed to proceed for 10 h. After that, the supernatant was collected by centrifugation (3 min at ~10000 rpm). Then supernatant was gradually evaporated at room temperature. After approximately 5~6 days, few square black crystals were harvested (18.7 % based on $PhCH_2SAg$).

Preparation of $[PdAg_{35}(PhCH_2S)_{18}(CF_3COO)_{10}(DMF)_4(PPh_3)_2]\cdot 10DMF\cdot 2H_2O$.

Firstly, $PhCH_2SAg$ (0.2 g, 0.9 mmol), CF_3COOAg (0.3 g, 1.4 mmol) were dissolved in a mixed solvent of CH_2Cl_2 and DMF (1:1). Then, $Ag^I(PPh_3)NO_3$ (0.4 g, 0.9 mmol) were added to the above solution, after 30 minutes, 3-bdppmapy (0.2 g, 0.4 mmol), $Pd(PPh_3)_4$ (0.46 g, 0.4 mmol) and 10 μL NEt_3 were added to the above mixture. The reaction was allowed to proceed for 10 h. After that, the supernatant was collected by centrifugation (3 min at ~10000 rpm). Then supernatant was gradually evaporated at room temperature. After approximately 5~6 days, few square black crystals were harvested (10.5 % based on $PhCH_2SAg$).

Detection of $^1O_2$.

4 mg DMA dissolved in 12 ml ethanol were used as stock solution. Before test, 1 ml D_2O were added into 2 ml stock solution, which makes the final test solution. Then, we put 0.4 mmol nanoclusters into the solution, and monitored each nanocluster with a fluorescence spectrometer under light irradiation.

Calculations Details

The calculations were performed using the semiempirical quantum mechanical methods

GFN1-xTB packages.[6-8] The single crystal structure was chosen as initial guess for ground state optimization at tight level. The optimized structure of the clusters preserved the basic characteristics of the input structure, only with slightly change in the bond length, bond angles and dihedral angles, which confirming the feasibility of GFN1-xTB methods for cluster calculations. The UV-Vis spectra were calculated by sTDA.[9, 10]

Supporting Figures

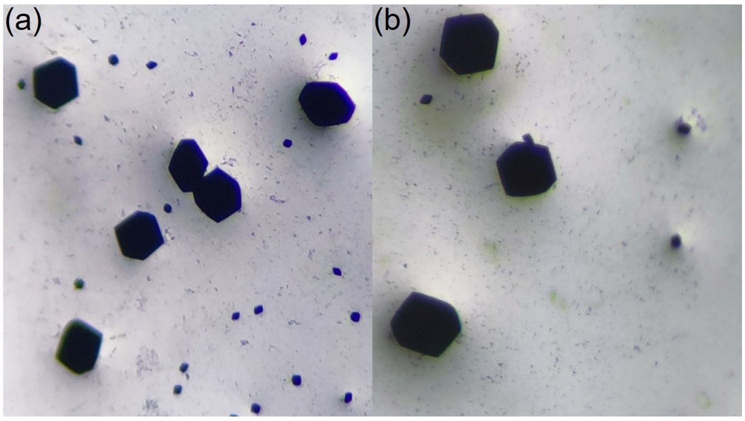

Figure S1. Photographs for crystals of (a) **Ag$_{36}$**, (b) **PdAg$_{35}$**.

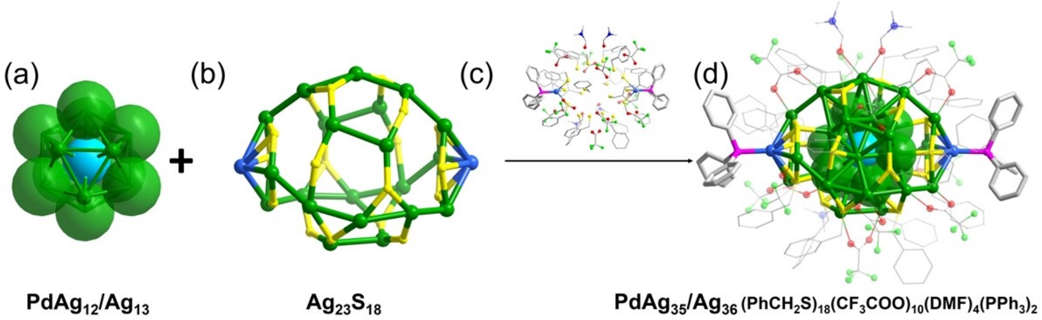

Figure S2. Anatomy of the structure of **Ag$_{36}$ (PdAg$_{35}$)**. (a) Ag$_{13}$ (PdAg$_{12}$) centered icosahedral core; (b) simplified shell with omit the CF$_3$COO$^-$, DMF and PPh$_3$ ligands; (c) the CF$_3$COO$^-$, DMF and PPh$_3$ ligands and their arrangement; (d) The overall structure of **Ag$_{36}$ (PdAg$_{35}$)**. Color codes: green and light blue, Ag; turquiose, Pd; yellow, S; red, O; purple, P; light green, F; blue, N; gray, C. For clarity, all H atoms are omitted.

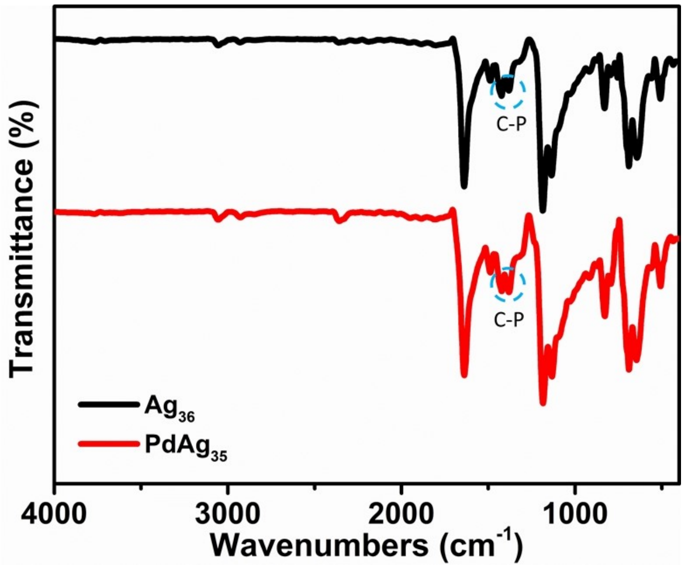

Figure S3. FT-IR spectra of **Ag$_{36}$**, **PdAg$_{35}$**.

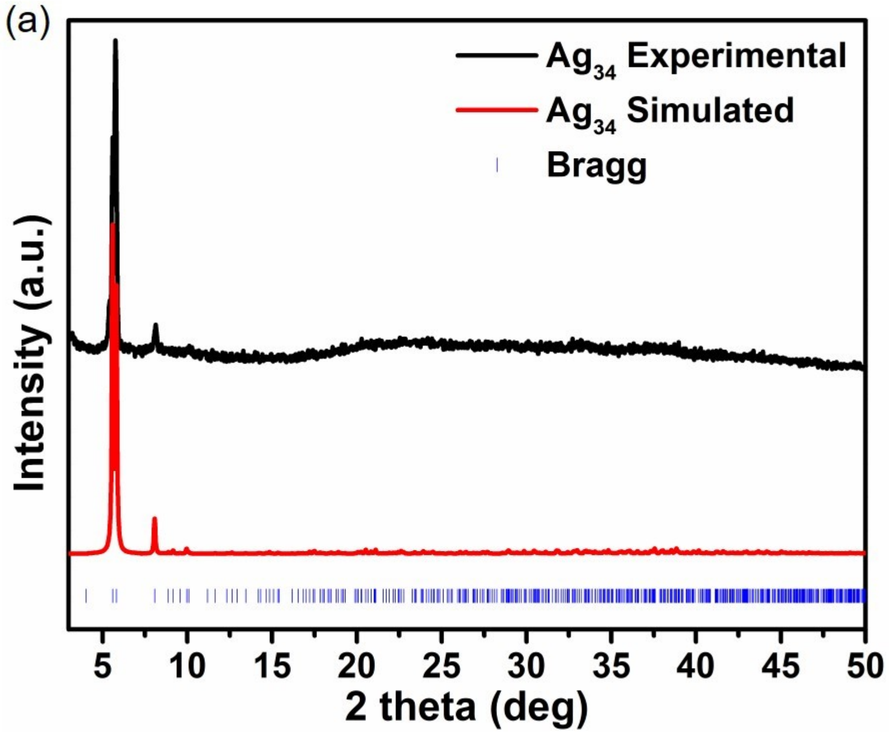
(a)
Ag$_{34}$ Experimental
Ag$_{34}$ Simulated
Bragg
Intensity (a.u.)
5
10
15
20
25
30
35
40
45
50
2 theta (deg)

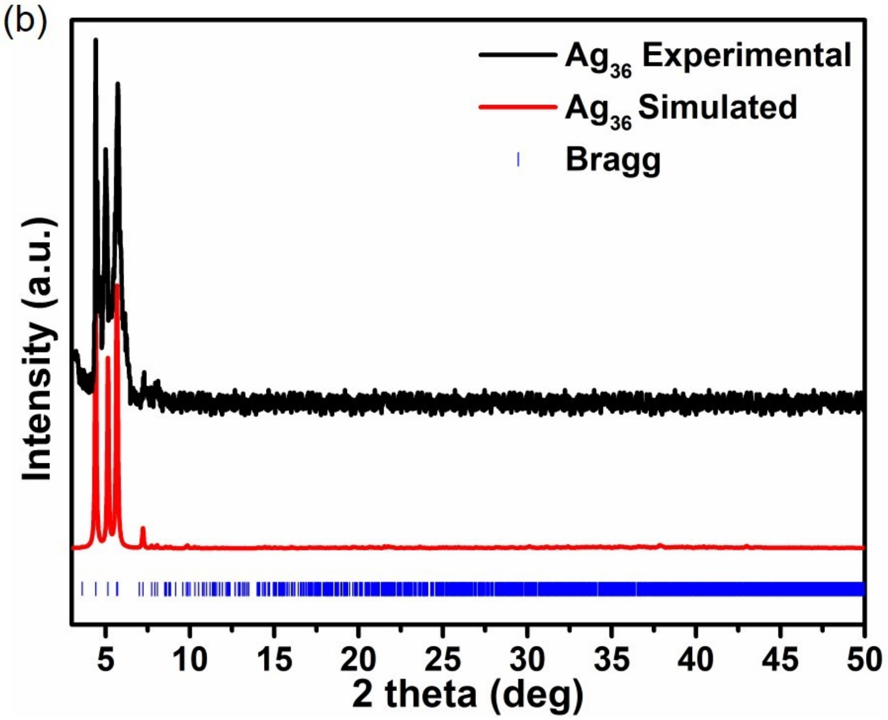
(b)
Ag$_{36}$ Experimental
Ag$_{36}$ Simulated
Bragg
Intensity (a.u.)
5
10
15
20
25
30
35
40
45
50
2 theta (deg)

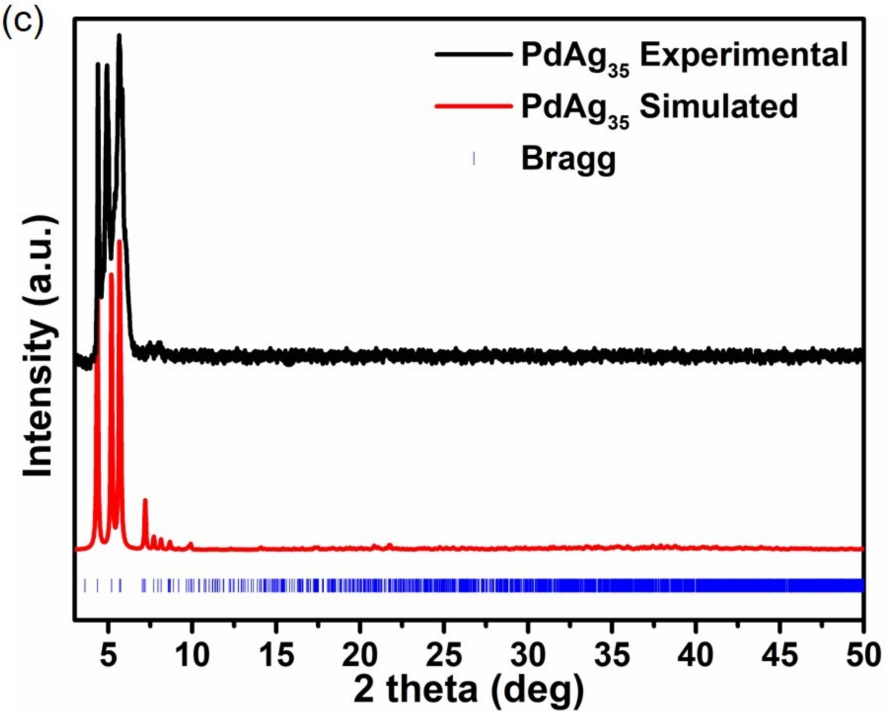

Figure S4. PXRD spectra of (a) **Ag_{34},** (b) **Ag_{36}** and (c) **$PdAg_{35}$**.

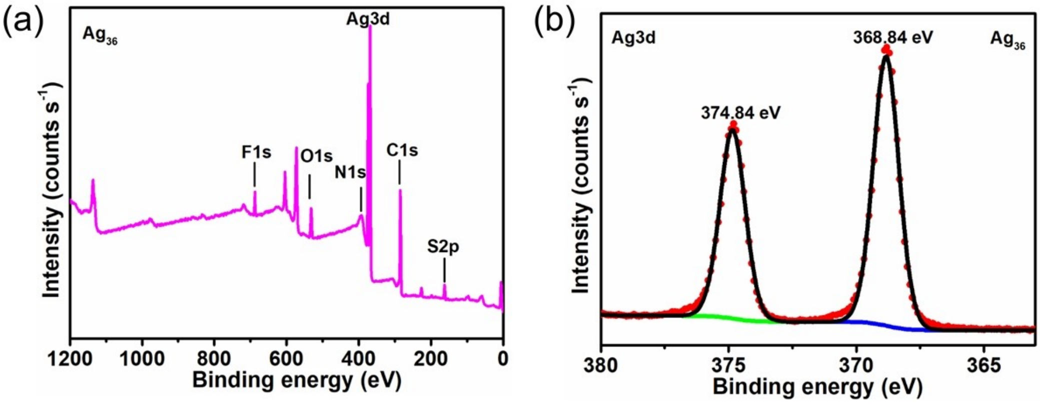

Figure S5. (a) XPS survey scan of **Ag_{36}**; (b) Ag 3d XPS spectra of **Ag_{36}**.

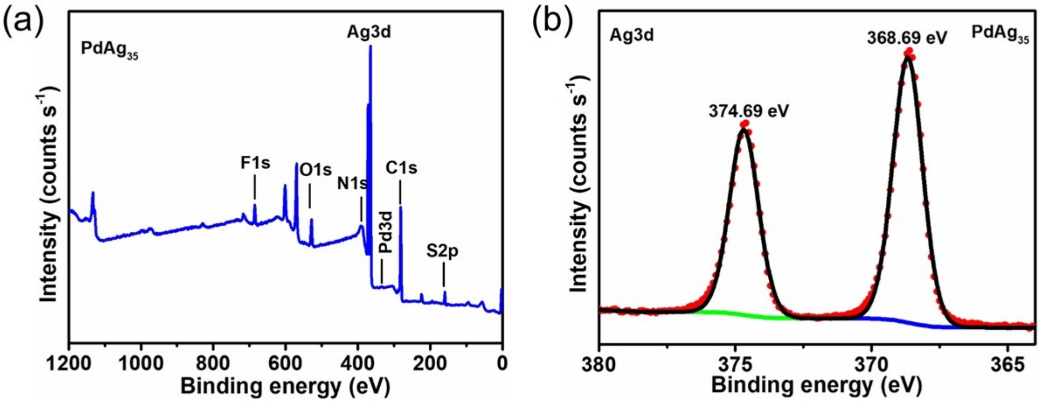

Figure S6. (a) XPS survey scan of **$PdAg_{35}$**; (b) Ag 3d XPS spectra of **$PdAg_{35}$**.

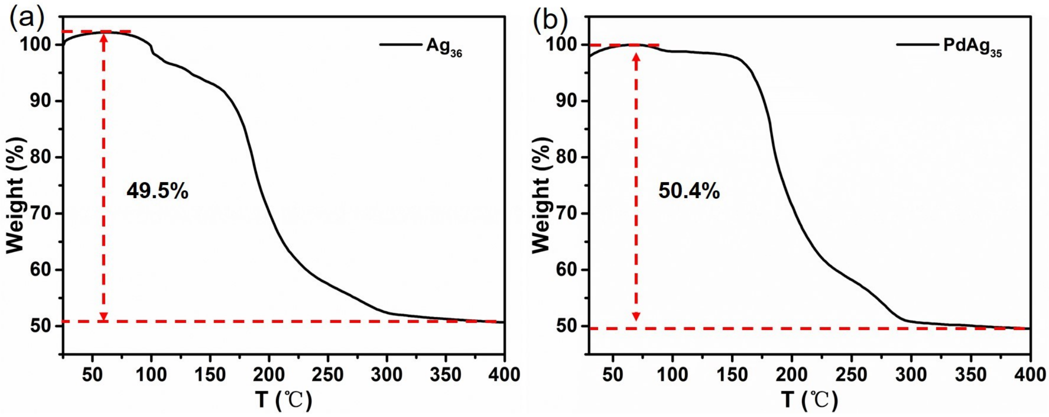

Figure S7. Thermogravimetric analysis (TGA) of as-synthesized (a) **Ag$_{36}$** and (b) **PdAg$_{35}$** under O_2 atmosphere.

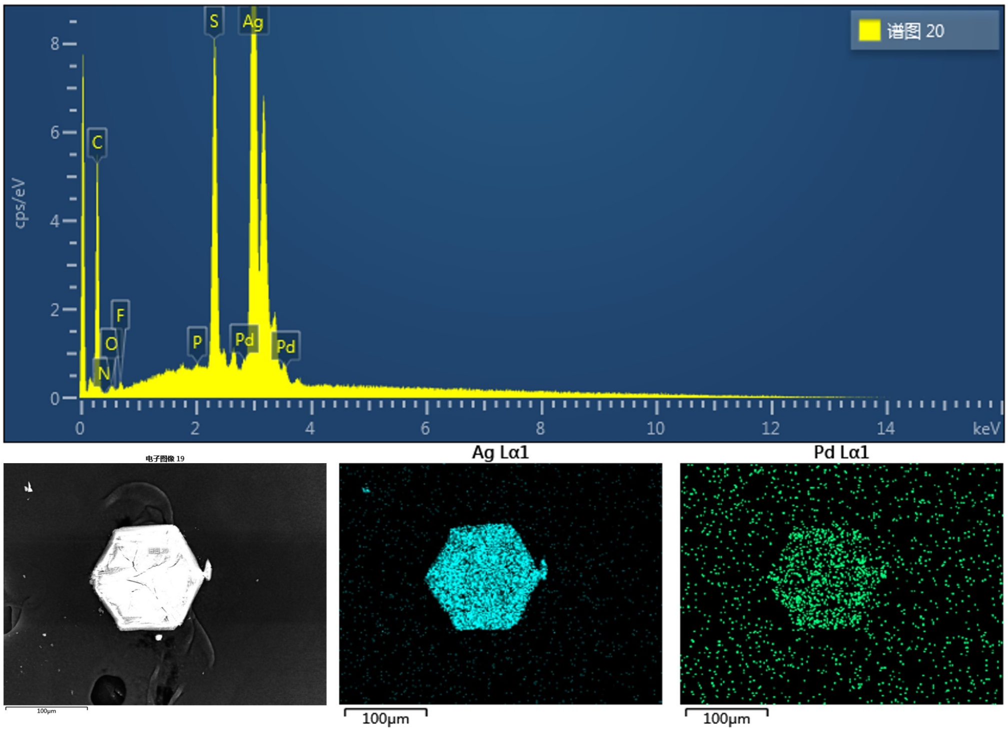

Figure S8. Morphologies of single crystals and energy dispersive spectroscopy (EDS) mapping results of **PdAg$_{35}$**.

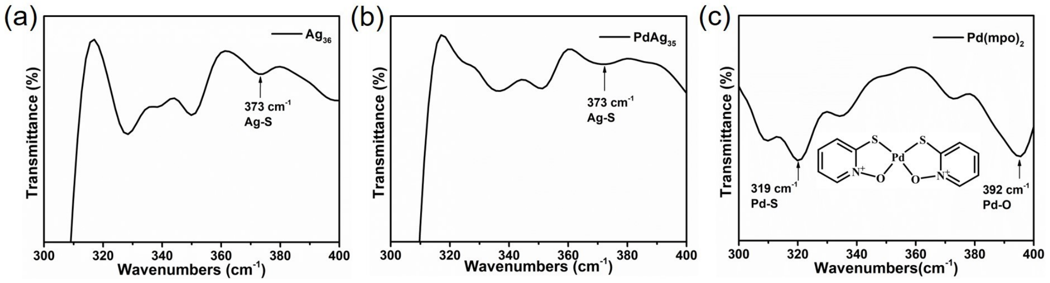

Figure S9. Far-IR spectra of (a) **Ag$_{36}$**; (b) **PdAg$_{35}$**; (c) Pd(mpo)$_2$.

The far-IR spectra of **Ag$_{36}$**, **PdAg$_{35}$** and model compound Pd(mpo)$_2$ (mpo = 2-mercaptopyridine N-oxide) further support the rationality assignment of the crystal structures. The far-IR spectra of Pd(mpo)$_2$ clearly shows the bands centered at 319 and 392 cm^{-1}, which are corresponding to the Pd-S and Pd-O, respectively[11]. By comparison, these bond peaks are absent in **PdAg$_{35}$**.

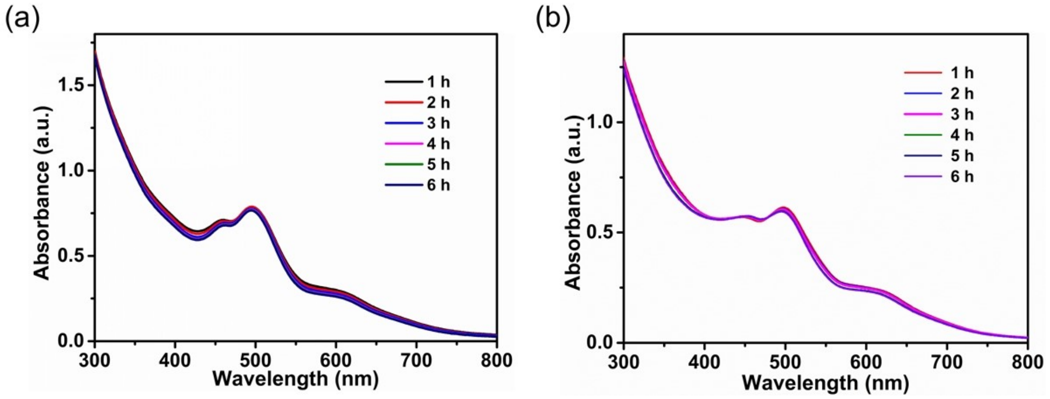

Figure S10. Time-dependent UV-vis spectra of (a) **Ag$_{36}$,** (b) **PdAg$_{35}$** in CH_2Cl_2 solution.

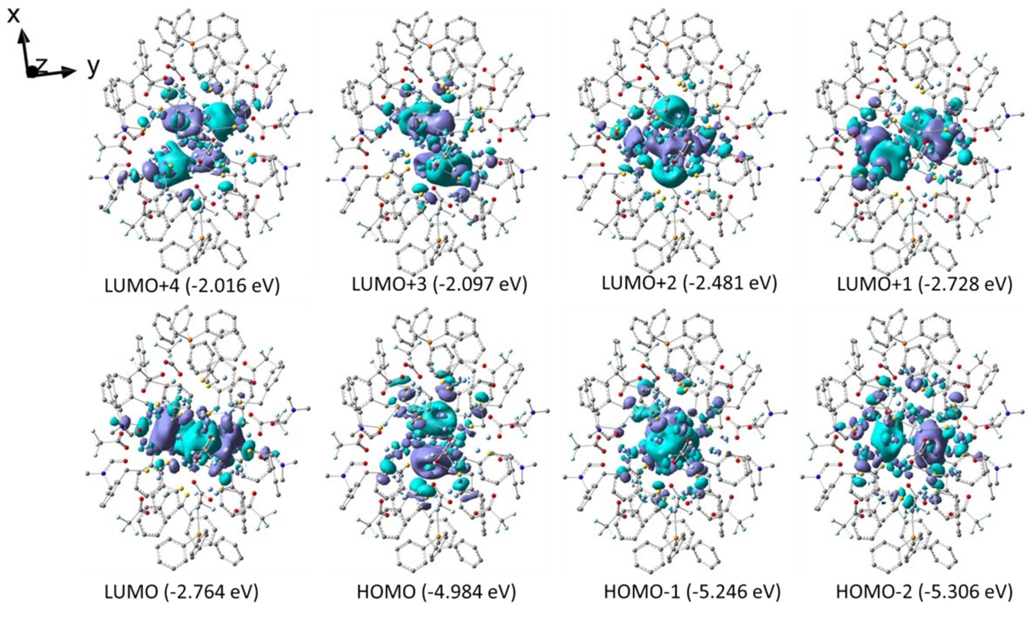

Figure S11. Selected molecular orbitals of the **Ag$_{36}$** nanocluster. Color codes: light blue, Ag; yellow, S; red, O; orange, P; cyan, F; blue, N; gray, C. For clarity, all H atoms are omitted.

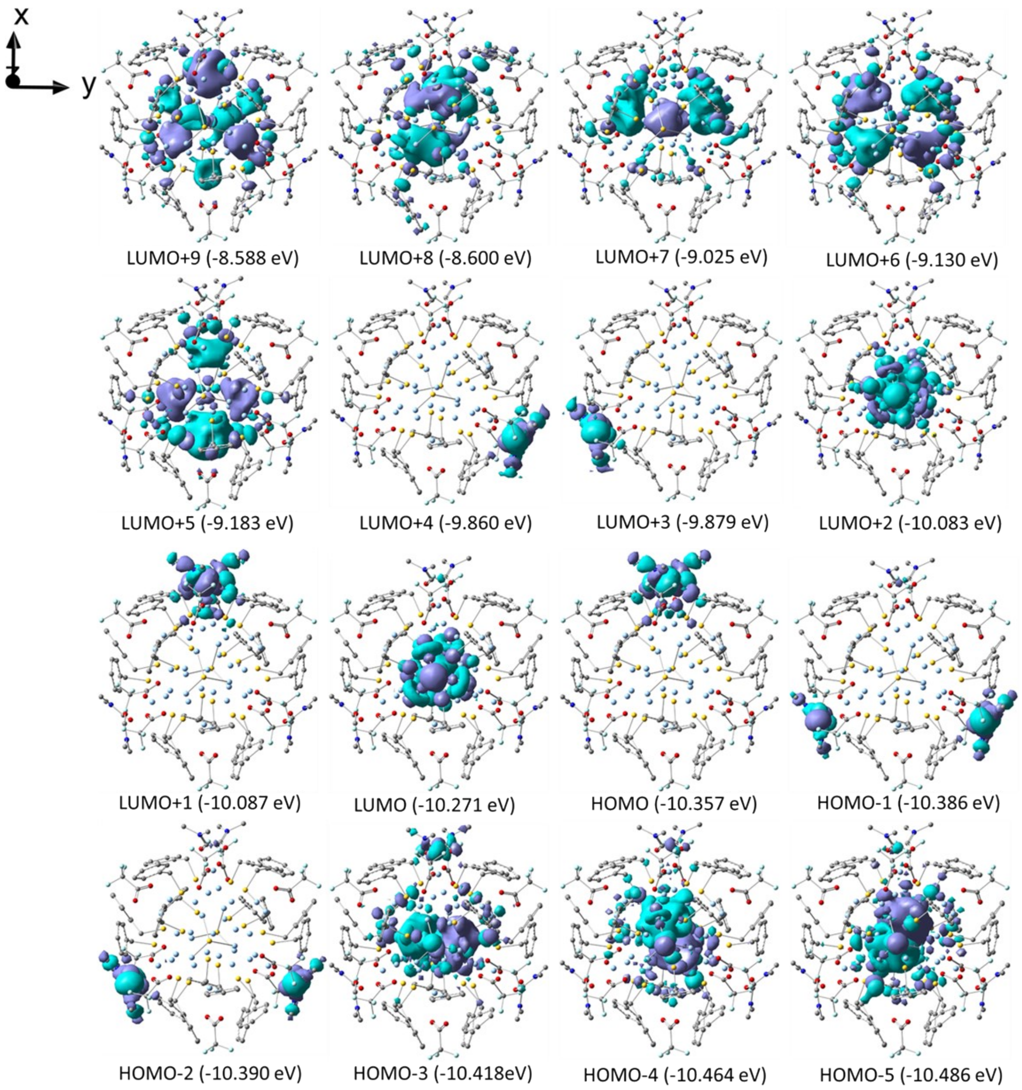

Figure S12. Selected α molecular orbitals of the **Ag$_{34}$** nanocluster. Color codes: light blue, Ag; yellow, S; red, O; cyan, F; blue, N; gray, C. For clarity, all H atoms are omitted.

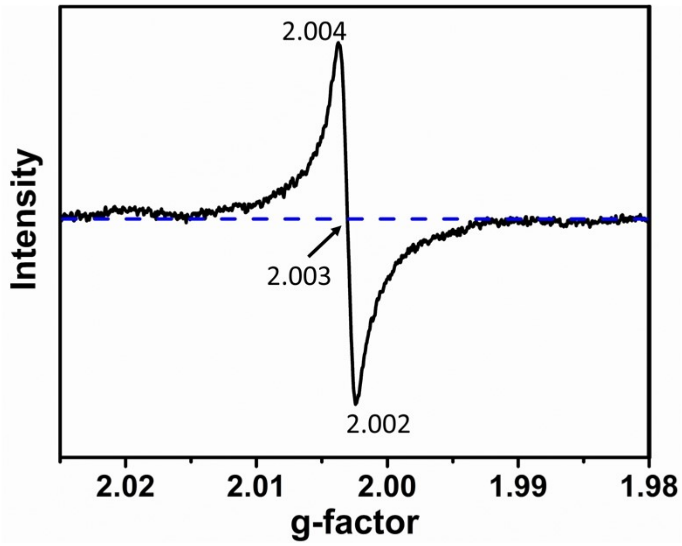

Figure S13. EPR spectra of **PdAg$_{35}$**.

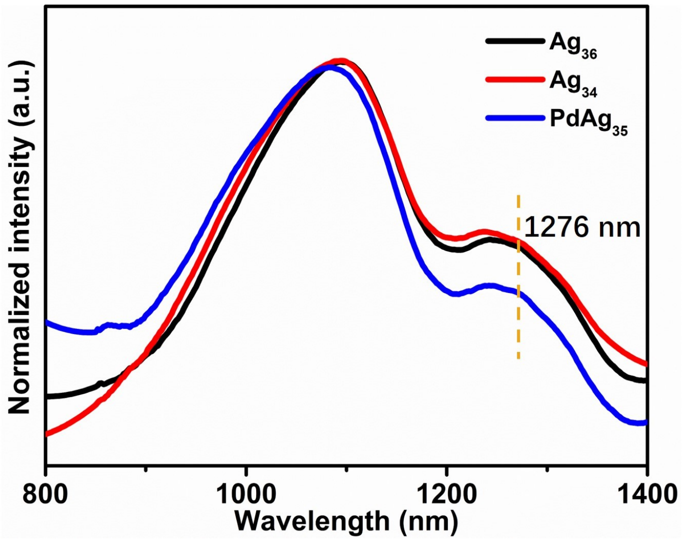

Figure S14. NIR spectra of **Ag_{34}**, **Ag_{36}** and **$PdAg_{35}$**.

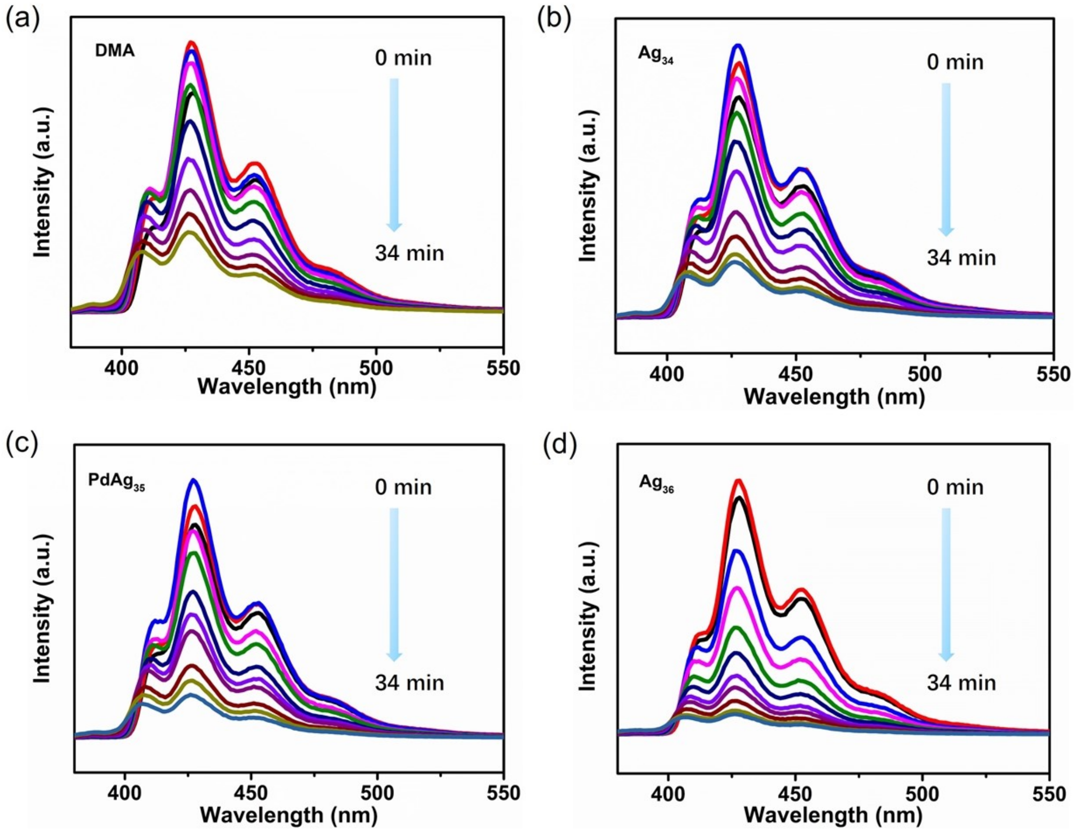

Figure S15. Comparison of the fluorescence intensity of DMA quenched by singlet oxygen of (a) DMA (blank); (b) DMA+**Ag_{34}**; (c) DMA+**$PdAg_{35}$**; (d) DMA+ **Ag_{36}**; in 2 ml EtOH and 1 ml D_2O (excited at 300 nm).

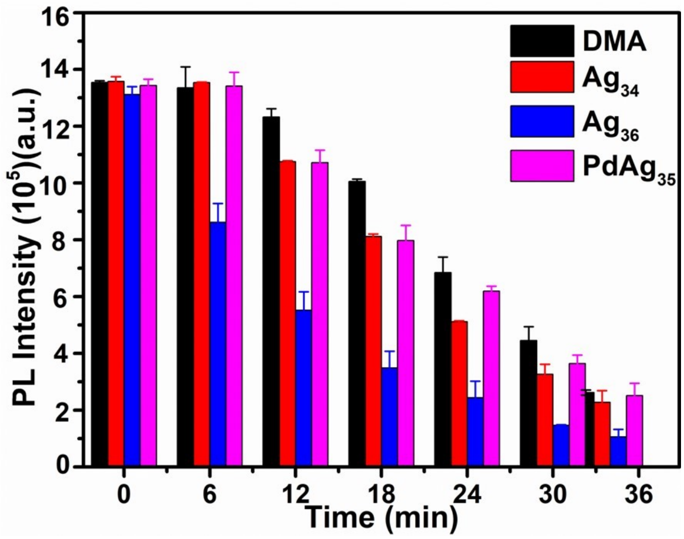

Figure S16. Comparison of rates of degradation of DMA using **Ag_{34}**, **$PdAg_{35}$** and **Ag_{36}** monitored by emission decay at 427 nm.

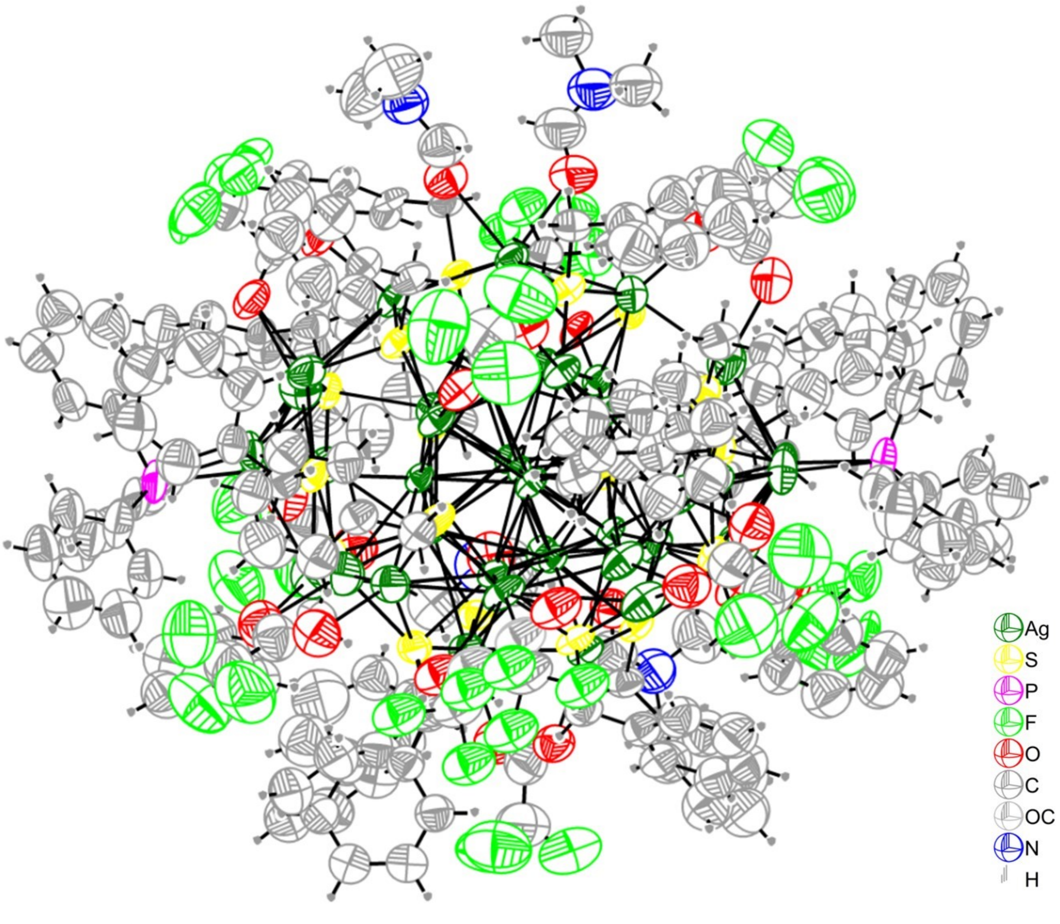

Figure S17. The ADP structure of **Ag_{36}**.

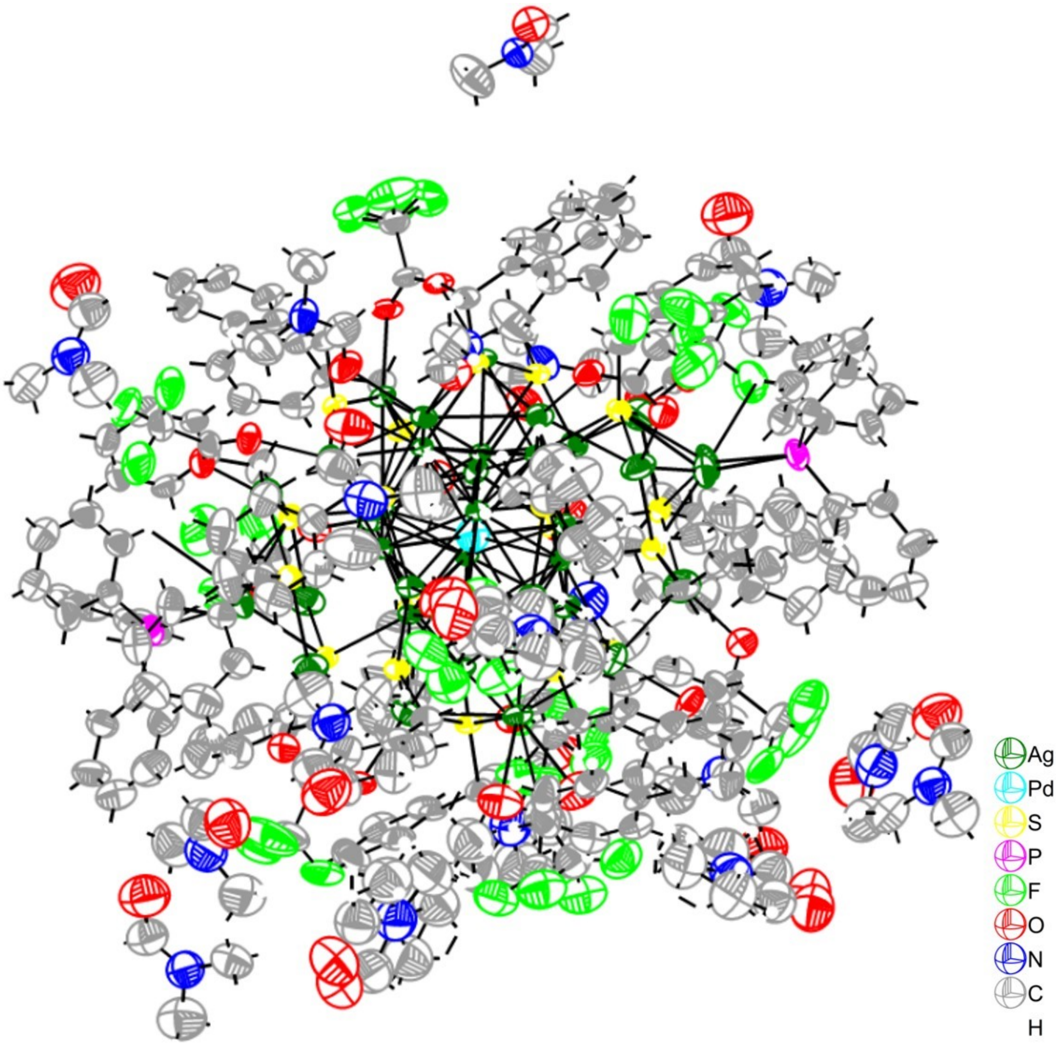

Figure S18. The ADP structure of **PdAg$_{35}$**.

Supporting Tables

Table S1. The atom ratio of **$PdAg_{35}$** nanoclusters calculated from inductively coupled plasma (ICP) measurements.

	Pd atom	Ag atom
ICP Experiment ratio of $PdAg_{35}$	2.91%	97.09%
Theoretical ratio of $PdAg_{35}$	2.78%	97.22%

Table S2. Comparison of bond lengths in **Ag_{34}** , **Ag_{36} and $PdAg_{35}$** clusters.

	Ag_{34}	**Ag_{36}**	**$PdAg_{35}$**
M_{cen}-M_{ico}	2.796-2.807 Å (average: 2.802 Å)	2.800-2.820 Å (average: 2.810 Å)	2.794-2.810 Å (average: 2.804 Å)
Ag_{ico}-Ag_{ico}	2.874-3.097 Å (average: 2.947 Å)	2.898-3.290 Å (average: 2.997 Å)	2.890-3.108 Å (average: 2.988 Å)
Ag_{ico}-S	2.508-2.578 Å (average: 2.543 Å)	2.514-2.598 Å (average: 2.560 Å)	2.520-2.591 Å (average: 2.562 Å)

Table S3. Comparisons of bond lengths in M_{13} icosahedron with the similar structures in the reported nanocluster.

Molecular formula	Icosahedron core[a]	Bond length (Å)		Refs
		M_{cen}.-M_{ico}[b]	M_{ico}.-M_{ico}	
$Ag_{36}(SR)_{18}(CF_3COO)_{10}$-$(DMF)_4(TPP)_2$	$Ag_{12}[Ag]$	2.80-2.82	2.89-3.29	This work
$PdAg_{35}(SR)_{18}(CF_3COO)_{10}$-$(DMF)_4(TPP)_2$	$Ag_{12}[Pd]$	2.79-2.81	2.89-3.11	This work
$Ag_{34}S_2(SR)_{18}(CF_3COO)_9$-$(DMF)_6$	$Ag_{12}[Ag]$	2.80-2.81	2.87-3.10	[5]
$Ag_{33}(SR)_{24}(PPh)_4$	$Ag_{12}[Ag]$	2.78-2.80	2.82-3.08	[12]
$Ag_{24}Pd(SR)_{18}$	$Ag_{12}[Pd]$	2.73-2.77	2.82-2.97	[13, 14]
$Ag_{24}Pt(SR)_{19}$	$Ag_{12}[Pt]$	2.73-2.78	2.83-3.00	[13, 14]
$Ag_{25}(SR)_{18}$	$Ag_{12}[Ag]$	2.72-2.79	2.82-3.00	[15]
$Ag_{24}Au(SR)_{18}$	$Ag_{12}[Au]$	2.74-2.80	2.86-2.98	[14, 16]
$Ag_{29}(BDT)_{12}(TPP)_4$	$Ag_{12}[Ag]$	2.75-2.77	2.83-2.97	[17]
$Au_{25}(SR)_{18}$	$Au_{12}[Au]$	2.76-2.79	2.80-2.99	[18, 19]

[a]. The icosahedron structure is formatted by the atoms compositions. Centered atom in the icosahedron is bracketed by [ ] for distinguishing.

[b]. A_{cen} and A_{ico} denote the centered atom in the icosahedron and atom on the vertex of the icosahedron, respectively.

Table S4. Crystallographic data and structure refinement for **Ag$_{36}$** and **PdAg$_{35}$**.

Identification code	**Ag$_{36}$**	**PdAg$_{35}$**
CCDC number	2150327	2150328
Empirical formula	$C_{224}H_{258}Ag_{36}F_{30}N_{14}O_{36}P_2S_{18}$	$C_{224}H_{258}Ag_{35}F_{30}N_{14}O_{36}P_2Pd_1S_{18}$
Formula weight	8814.77	8813.30
Temperature/K	200.00(10)	199.99(10)
Crystal system	monoclinic	monoclinic
Space group	*C*2/*c*	*C*2/*c*
a/Å	40.552(10)	41.1371(3)
b/Å	30.945(7)	30.7832(2)
c/Å	22.193(5)	21.93730(10)
α/°	90	90
β/°	99.116(12)	98.3850(10)
γ/°	90	90
Volume/Å^3	27497(11)	27482.9(3)
Z	4	4
ρ_{calc}g/cm^3	2.129	2.130
μ/mm^{-1}	2.727	22.094
F(000)	17072.0	17068.0
Crystal size/mm^3	0.13 × 0.12 × 0.1	0.3 × 0.2 × 0.2
Radiation	Mo Kα (λ = 0.71073)	Cu Ka (λ = 1.54184)
2θ range for data collection/°	3.922 to 50	4.342 to 148.29
Index ranges	$-48 \leq h \leq 48$, $-36 \leq k \leq 36$, $-26 \leq l \leq 26$	$-46 \leq h \leq 51$, $-37 \leq k \leq 23$, $-22 \leq l \leq 26$
Reflections collected	650255	75567
Independent reflections	24206 [R_{int} = 0.1231, R_{sigma} = 0.0332]	27045 [R_{int} = 0.0636, R_{sigma} = 0.0545]
Data/restraints/parameters	24206/1100/1414	27045/446/1687
Goodness-of-fit on F^2	1.134	1.060
Final R indexes [I>=2σ (I)]	R_1 = 0.0959, wR_2 = 0.2080	R_1 = 0.0722, wR_2 = 0.1877
Final R indexes [all data]	R_1 = 0.1400, wR_2 = 0.2606	R_1 = 0.0906, wR_2 = 0.2066
Largest diff. peak/hole/e Å^{-3}	2.18/-1.89	2.53/-3.27

Supplementary Reference.

1. J.-F. Wang, S.-Y. Liu, C.-Y. Liu, Z.-G. Ren and J.-P. Lang, *Dalton Trans.*, 2016, **45**, 9294-9306.
2. G. M. Sheldrick, *Acta Crystallogr C Struct Chem*, 2015, **71**, 3-8.
3. A. Spek, *Acta Crystallographica Section D*, 2009, **65**, 148-155.
4. X. Kang, X. Wei, S. Jin, Q. Yuan, X. Luan, Y. Pei, S. Wang, M. Zhu and R. Jin, *Proceedings of the National Academy of Sciences*, 2019, **116**, 18834.
5. X.-J. Xi, J.-S. Yang, J.-Y. Wang, X.-Y. Dong and S.-Q. Zang, *Nanoscale*, 2018, **10**, 21013-21018.
6. C. Bannwarth, E. Caldeweyher, S. Ehlert, A. Hansen, P. Pracht, J. Seibert, S. Spicher and S. Grimme, *WIREs Computational Molecular Science*, 2020, **11**.
7. C. Bannwarth, S. Ehlert and S. Grimme, *J. Chem. Theory Comput.*, 2019, **15**, 1652-1671.
8. S. Grimme, C. Bannwarth and P. Shushkov, *J. Chem. Theory Comput.*, 2017, **13**, 1989-2009.
9. S. Grimme, *J. Chem. Phys.*, 2013, **138**, 244104.
10. S. Grimme and C. Bannwarth, *J. Chem. Phys.*, 2016, **145**, 054103.
11. J.-C., Shi; Thomas C. W. Mak , Polyhedron, 1997, 16, 369−375.
12. F. Tian and R. Chen, *J. Am. Chem. Soc.*, 2019, **141**, 7107-7114.
13. J. Yan, H. Su, H. Yang, S. Malola, S. Lin, H. Häkkinen and N. Zheng, *J. Am. Chem. Soc.*, 2015, **137**, 11880-11883.
14. X. Liu, J. Yuan, C. Yao, J. Chen, L. Li, X. Bao, J. Yang and Z. Wu, *The Journal of Physical Chemistry C*, 2017, **121**, 13848-13853.
15. C. P. Joshi, M. S. Bootharaju, M. J. Alhilaly and O. M. Bakr, *J. Am. Chem. Soc.*, 2015, **137**, 11578-11581.
16. M. S. Bootharaju, C. P. Joshi, M. R. Parida, O. F. Mohammed and O. M. Bakr, *Angew. Chem. Int. Ed. Engl.*, 2016, **55**, 922-926.
17. L. G. AbdulHalim, M. S. Bootharaju, Q. Tang, S. Del Gobbo, R. G. AbdulHalim, M. Eddaoudi, D. E. Jiang and O. M. Bakr, *J. Am. Chem. Soc.*, 2015, **137**, 11970-11975.
18. M. W. Heaven, A. Dass, P. S. White, K. M. Holt and R. W. Murray, *J. Am. Chem. Soc.*, 2008, **130**, 3754-3755.
19. M. Zhu, C. M. Aikens, F. J. Hollander, G. C. Schatz and R. Jin, *J. Am. Chem. Soc.*, 2008, **130**, 5883-5885.